NON-MAXWELLIAN ION DISTRIBUTIONS IN THE IONIZATION ZONE OF THE TOKAMAK BOUNDARY

G. Becker

IPP III/69 Mai 1981

MAX-PLANCK-INSTITUT FÜR PLASMAPHYSIK

8046 GARCHING BEI MÜNCHEN

MAX-PLANCK-INSTITUT FÜR PLASMAPHYSIK

GARCHING BEI MÜNCHEN

NON-MAXWELLIAN ION DISTRIBUTIONS IN THE IONIZATION ZONE OF THE TOKAMAK BOUNDARY

G. Becker

IPP III/69 Mai 1981

Die nachstehende Arbeit wurde im Rahmen des Vertrages zwischen dem Max-Planck-Institut für Plasmaphysik und der Europäischen Atomgemeinschaft über die Zusammenarbeit auf dem Gebiete der Plasmaphysik durchgeführt.

IPP III/69 G. Becker

NON-MAXWELLIAN ION DISTRIBUTIONS IN THE IONIZATION ZONE OF THE TOKAMAK BOUNDARY

May 1981
(in English)

ABSTRACT: Steady-state ion guiding-centre distributions are computed for the ionization zone of the tokamak boundary by numerically solving the drift-kinetic equation with Coulomb ion-ion and electron-ion collision terms and with sources and sinks due to ionization of and charge exchange with neutrals from the walls. For typical temperatures $T_e = T_i \gtrsim 50$ to 100 eV and $\frac{n_o}{n} \gtrsim 2 \cdot 10^{-4}$ to 10^{-3} one obtains marked deviations from Maxwellian distributions that grow with increasing $\frac{n_o}{n}$ and $\frac{T_i}{T_o}$. Both ionization and charge exchange can produce large distortions which possibly cause microinstabilities in the boundary. For $T_e \approx T_i$ the contributions of electron-ion collisions to the ion collision term are in the range of a few per cent. The relaxation time to steady-state exceeds the classical ion-ion collision time by about a factor of 4.

1. INTRODUCTION

It is well known that the plasma boundary belongs to the catalogue of problems which have to be solved for successful development of a fusion reactor. Undoubtedly, the boundary region is of outstanding importance, e.g. for particle and energy balances, production and transport of impurities, fuel injection (recycling, gas puffing, neutral injection), ash removal and plasma heating (neutral injection heating, HF heating).

Up to now there has been no self-consistent treatment of the essential boundary problems of tokamaks by one computational model. In the present situation models for the investigation of special questions of the plasma edge which promise more insight into the physical processes involved are appropriate and useful. One such problem is the turbulence of the plasma boundary (typical edge parameters $T_e \approx T_i \approx 20 - 100$ eV, $n \lesssim 10^{13}$ cm^{-3}) observed in many tokamaks. The measured anomalously high diffusion rates [1-3] and large density and potential fluctuations levels ($\frac{\tilde{n}}{n} \approx \frac{e\tilde{\Phi}}{kT_e} \approx 0.1 - 0.4$) [4] are ascribed to as yet unidentified instabilities, presumably microinstabilities [5]. In the boundary region steady-state differences between the ion distribution functions f and the Maxwellian f_M that could drive velocity space instabilities are maintained by drifts and temperature gradients, by sources and sinks for particles and energy due to ionization of and charge exchange with neutrals from limiters and walls or by velocity-dependent ion losses. The magnitude of the distortion of the Maxwellian ion velocity distribution is determined by the intensity and $\vec{v}$-dependence of sources and sinks as well as by velocity-space diffusion.

Obviously, a kinetic computer model is needed in order to describe quantitatively these processes. A lower limit for the relaxation of the distributions is set by classical diffusion in velocity space and can be described by the Fokker-Planck operator for binary (ion-ion) collisions.

The main purpose of the present paper is to use a Fokker-Planck computer model for the ions to investigate which processes in the tokamak boundary are able to produce significant distortions of the Maxwellian ion distribution and serve as possible causes of microinstabilities. One objective is to determine the parameters and conditions in the ionization zone forwhich marked deviations from Maxwellians occur in the presence of sources and sinks for particles and energy on the one hand and classical velocity-space diffusion on the other. Moreover, we are interested in the limitations of the usual fluid description of the ions in the tokamak boundary and in prediction (by extrapolating 2 D results) of the execution time and storage capacity needed, e.g. for a 4 D Fokker-Planck boundary code with two space and two velocity variables.

These aims are pursued for the ionization zone of the tokamak boundary by modelling the ions (i) by the drift-kinetic equation, i.e. the Fokker-Planck-equation, ordered in the gyroradius and averaged over the gyrophase [6]. We include the complete nonlinear Fokker-Planck operator for ion-ion and ion-electron collisions. The electrons (e) are described as a fluid in thermal equilibrium, whereas for the neutrals (o) various distribution functions can be prescribed. Sources and sinks due to electron impact ionization and charge exchange are taken into account. The inclusion of cross-field diffusion would require in addition a two-dimensional space grid. Diffusion is simulated instead by a numerical correction of f which provides for conservation of particle number and energy and allows for stationary solutions. The actual mathematical model is presented in section 2. In section 3 calculated steady-state ion distributions for various parameters in the ionization zone are presented and discussed. Although the computations are done with typical parameters of the tokamak boundary, the results hold more generally for plasmas with similar data interacting with neutrals from the walls.

/3

2. MODEL

In this section we begin with the assumptions of the Fokker-Planck model for the ionization zone of the boundary. We then describe the drift-kinetic equation solved and the boundary conditions used and, finally, make a few remarks on the numerical methods.

2.1 BASIC ASSUMPTIONS

For typical plasma densities and temperatures in the limiter shadow of tokamaks [1,7] the mean free paths for ionization and charge exchange of D atoms from the wall are large compared with the thickness of the limiter shadow region. Thus, the real ionization and charge exchange zone lies in the denser and hotter plasma at radii smaller than the limiter radius.
We therefore assume edge parameters for which the neutral particle distribution function $f_o(\vec{v})$ at the walls and limiters is not changed much by ionization, charge exchange and elastic collisions between neutrals and ions before the neutrals reach the ionization zone.
In the ionization zone there are no ion losses $\parallel \vec{B}$, so that under steady-state conditions the ion sources are compensated by cross-field diffusion alone.
By contrast, the scrape-off layer exhibits only weak ion sources but considerable losses $\parallel \vec{B}$. For these and other reasons it is reasonable to separate the ionization zone from the scrape-off layer.

2.2 DRIFT-KINETIC EQUATION WITH SOURCES AND SINKS

If excessively large execution times even on fast computers are to be avoided, several simplifications are necessary in the general transport equation for the ions, the Fokker-Planck-equation

$$\frac{\partial f}{\partial t} + \vec{v} \cdot \frac{\partial f}{\partial \vec{r}} + \vec{a} \cdot \frac{\partial f}{\partial \vec{v}} = \left(\frac{\partial f}{\partial t}\right)_c$$

where $\vec{v} = \frac{d\vec{r}}{dt}$ and $\vec{a} = \frac{d\vec{v}}{dt}$. In velocity space we use the

spherical coordinates v, θ, ζ for the velocity, the pitch angle and the gyrophase angle, respectively. By ordering with respect to the gyroradius and averaging over ζ the Fokker-Planck equation can be reduced to the drift-kinetic equation governing the distribution of guiding-centres [6]. After adding source and sink functions S one obtains

$$\frac{\partial f}{\partial t} + (\vec{v}_{\parallel} + \vec{v}_{d}) \cdot \vec{\nabla} f = \left(\frac{\partial f}{\partial t}\right)_c + S \quad . \tag{1}$$

Here the time derivatives of the electrostatic potential and the vector potential have been set equal to zero. Even in the axially symmetric case the solutions of Eq.(1) still depend on two space and two velocity variables, so that a numerical solution would only be possible on a very coarse grid. Consequently, in a first approach we further simplify the equation by assuming spatial homogeneity and simulate the losses due to diffusion by a sink term S_d. Thus, we finally obtain

$$\frac{\partial f}{\partial t} = \left(\frac{\partial f}{\partial t}\right)_c + S + S_d \quad . \tag{2}$$

The nonlinear ion Fokker-Planck collision operator for ion-ion and ion-electron collisions is given by [8,9]

$$\begin{aligned}
\frac{1}{\Gamma}\left(\frac{\partial f}{\partial t}\right)_c = {} & \frac{1}{2}\frac{\partial^2 g}{\partial v^2}\frac{\partial^2 f}{\partial v^2} + \frac{1}{v^2}\left(\frac{\partial^2 g}{\partial v \partial \theta} - \frac{1}{v}\frac{\partial g}{\partial \theta}\right)\frac{\partial^2 f}{\partial v \partial \theta} \\
& + \frac{1}{2}\frac{1}{v^3}\left(\frac{1}{v}\frac{\partial^2 g}{\partial \theta^2} + \frac{\partial g}{\partial v}\right)\frac{\partial^2 f}{\partial \theta^2} \\
& + \frac{1}{v^2}\left(\frac{1}{2v}\frac{\partial^2 g}{\partial \theta^2} + \frac{1}{2v}\cot\theta\frac{\partial g}{\partial \theta} + \frac{\partial g}{\partial v}\right)\frac{\partial f}{\partial v} \\
& + \frac{1}{v^3}\left(\frac{1-\frac{1}{2}\cos^2\theta}{v\sin^2\theta}\frac{\partial g}{\partial \theta} - \frac{\partial^2 g}{\partial v \partial \theta} + \frac{1}{2}\cot\theta\frac{\partial g}{\partial v}\right)\frac{\partial f}{\partial \theta} \\
& + \frac{\partial C}{\partial v}\frac{\partial f}{\partial v} + \frac{1}{v^2}\frac{\partial C}{\partial \theta}\frac{\partial f}{\partial \theta} \\
& + 4\pi\left(\frac{m_i}{m_e} f_e + f\right) f \quad ,
\end{aligned} \tag{3}$$

where $\Gamma = 4\pi \left(\frac{e^2}{m_i}\right)^2 \ln\Lambda$ with the deuteron mass m_i and the Coulomb logarithm $\ln\Lambda$,

$$g = \int d^3\vec{v}' \left(f_e(\vec{v}') + f(\vec{v}')\right) |\vec{v} - \vec{v}'| \qquad \text{("Rosenbluth potential")},$$

$$C = \left(1 - \frac{m_i}{m_e}\right) \int d^3\vec{v}' f_e(\vec{v}') \, |\vec{v} - \vec{v}'|^{-1}.$$

In spherical coordinates g and C can be expressed by

$$g(v,\theta) = \int_0^\infty dv' v'^2 \int_0^\pi d\theta' \sin\theta' \left(f_e(v',\theta') + f(v',\theta')\right) M(v',\theta';v,\theta), \qquad (4)$$

$$C(v,\theta) = \left(1 - \frac{m_i}{m_e}\right) \int_0^\infty dv' v'^2 \int_0^\pi d\theta' \sin\theta' f_e(v',\theta') N(v',\theta';v,\theta), \qquad (5)$$

with

$$M = 4q\, E\left(\frac{p}{q}\right), \quad N = \frac{4}{q} K\left(\frac{p}{q}\right),$$

$$p = 2\left(v v' \sin\theta \sin\theta'\right)^{\frac{1}{2}},$$

$$q = \left(v^2 + v'^2 - 2 v v' \cos(\theta + \theta')\right)^{\frac{1}{2}},$$

where E and K are the complete elliptic integrals.

The source function S reads

$$S = f_0(\vec{v}) \langle \sigma_i v_e \rangle n + f_0(\vec{v}) \int d^3\vec{v}_0 \, |\vec{v} - \vec{v}_0| \, \sigma_{cx} f(\vec{v}_0)$$
$$- f(\vec{v}) \int d^3\vec{v}_0 \, |\vec{v} - \vec{v}_0| \, \sigma_{cx} f_0(\vec{v}_0). \qquad (6)$$

The first term is the electron impact ionization rate and the second and third terms describe charge exchange. For typical edge parameters the recombination rate is negligibly small compared with the charge exchange loss rate.
Since the cross-field diffusion simulated by numerical correction of f must compensate the source term due to ionization it is given by

$$S_d = -f(\vec{v}) \langle \sigma_i v_e \rangle n_o \quad . \tag{7}$$

We assume a neutral density n_o small compared with n, so that elastic collisions between ions and neutrals may be neglected.

Since Eq. (2) is solved after normalizing it with respect to n, the results obtained represent a whole family of solutions for various n with the parameters T_e, T_i, T_o and $\frac{n_o}{n}$.

The electron contribution to the ion collision operator can be considerably simplified by treating the electrons as a fluid in thermal equilibrium. With a Maxwellian distribution function for the electrons

$$f_e(\vec{v}) = n \left(\frac{m_e}{2\pi k T_e}\right)^{\frac{3}{2}} \exp\left(-\frac{m_e v^2}{2 k T_e}\right)$$

an analytical integration of the additional terms $\frac{\partial^2 g_e}{\partial v^2}$, $\frac{\partial g_e}{\partial v}$ and $\frac{\partial C}{\partial v}$ can be carried out.

As discussed above, the limiter shadow is permeable to neutrals from the walls. We assume that gas puffing (Franck-Condon neutrals with T_o = 3 eV) and recycling are the dominant mechanisms of neutral production. The neutral particle source resulting from backscattering of ions is not taken into account.

2.3 BOUNDARY AND INITIAL CONDITIONS

The previous equations have to be completed by a set of boundary conditions for v and Θ. In our calculations we use the conditions given in Eqs. (11) to (14) which can be justified by the transformation relations between Cartesian (v_x, v_y, v_z) and spherical (v, Θ, ζ) coordinates:

$$\frac{\partial f}{\partial v} = \frac{\partial f}{\partial v_x} \sin\Theta\cos\zeta + \frac{\partial f}{\partial v_y} \sin\Theta\sin\zeta + \frac{\partial f}{\partial v_z} \cos\Theta \qquad (8)$$

$$\frac{\partial f}{\partial \Theta} = \frac{\partial f}{\partial v_x} v\cos\Theta\cos\zeta + \frac{\partial f}{\partial v_y} v\cos\Theta\sin\zeta - \frac{\partial f}{\partial v_z} v\sin\Theta . \qquad (9)$$

From Eq. (8) one obtains

$$\frac{\partial f}{\partial v}(v=0,\Theta) = \frac{\partial f}{\partial v_z}(v_z=0)\cos\Theta . \qquad (10)$$

Here $v_x = v_y = v_z = 0$ at $v = 0$ and $\frac{\partial f}{\partial v_x}(v_x = o) = \frac{\partial f}{\partial v_y}(v_y = o) = 0$ for guiding-centre distributions (because of azimuthal symmetry and continuity of the derivatives) have been used. In the ionization zone $\frac{\partial f}{\partial v_z}(v_z = o) = 0$ is assumed yielding $\frac{\partial f}{\partial v}(v = o, \Theta) = 0$, which means that distributions with a v_z-drift superposed are excluded. For $\Theta = 0$ and π again $v_x = v_y = 0$ holds and $\frac{\partial f}{\partial \Theta}(v,\Theta=0) = \frac{\partial f}{\partial \Theta}(v,\Theta=\pi) = 0$ is obtained. With these assumptions the set of boundary conditions used reads

$$f(v\to\infty, \Theta) = 0 \qquad (11)$$

$$\frac{\partial f}{\partial v}(v = o, \Theta) = 0 \qquad (12)$$

$$\frac{\partial f}{\partial \Theta}(v, \Theta = 0) = 0 \qquad (13)$$

$$\frac{\partial f}{\partial \Theta}(v, \Theta = \pi) = 0 \qquad (14)$$

For $\Theta = \frac{\pi}{2}$ Eq. (10) yields $\frac{\partial f}{\partial v}(v = 0, \Theta = \frac{\pi}{2}) = 0$, which is a generally valid condition, because no assumptions about $\frac{\partial f}{\partial v_z}(v_z = o)$ have been made. Another general condition is that $f(v = o, \Theta)$ has to be independent of Θ, because $v = o$, Θ marks the same point in velocity space for all Θ.

By the same procedure one can derive

$$\frac{\partial g}{\partial v}\ (v = o, \Theta) = 0,$$

$$\frac{\partial g}{\partial \Theta}\ (v, \Theta = o) = 0,$$

$$\frac{\partial g}{\partial \Theta}\ (v, \Theta = \pi) = 0.$$

In addition to f (v = o, Θ), also g (v = o, Θ) has to be independent of Θ. Both conditions can be used to check the program.

In order to solve the time dependent drift-kinetic equation (Eq. (2)), it is necessary to prescribe an initial distribution function for the ions. Maxwellian distributions have proved to be adequate even in computations that yield steady-state solutions with strong distortions of Maxwellians.

2.4 NUMERICAL SOLUTION

The numerical integration of the drift-kinetic equation (Eq.(2)) is carried out by difference methods. An equidistant Eulerian grid for v and Θ is used with v ranging from O to 4 $\left(\frac{kT_i}{m_i}\right)^{\frac{1}{2}}$ and Θ from O to π. With this upper limit for the speed sufficiently precise higher velocity moments of f are obtained. Typically, 60 grid points for the speed and 20 grid points for the pitch angle are needed for convergence to stationary solutions.

A simple method of finding stationary solutions for f is to solve Eq.(2) with $\frac{\partial f}{\partial t}$ = o by means of test functions. It is convenient to use families of trial functions, e.g. two-temperature distributions, where one temperature acts as a parameter of the family of functions.

A more systematic tool for solving the drift-kinetic equation is the application of an explicit scheme. Since such schemes are numerically stable only for rather small time steps, a large number of steps is needed in order to approach the stationary solution for f. Numerical instability near v = 0 is avoided by correcting f in such a manner that the particle number and energy of the ions are conserved. This is done at each time step by multiplying f by a function $u_1 + u_2 v^2$, whose coefficients are determined from the relations for conservation of particles and energy [10]. As mentioned above this correction simulates cross-field diffusion and particle and energy sources or sinks ($S_d(\vec{v})$). The conservation laws for the Fokker-Planck collision operator are checked.

Most computations have been done with a fast 1 D code for isotropic distributions and 60 grid points in the v range. Typically, up to 10^3 to 10^4 time steps are needed until the stationary solution is reached, this corresponding to an execution time on an AMDAHL 470 computer of about 30 s. Convergence is only achieved with a sufficiently fine v grid if a stability criterion for the velocity step Δv and the time step Δt

$$\frac{\Delta t}{(\Delta v)^2} \leq \text{const}\ (T_i)$$

is fulfilled (analogous to the criterion by Richtmyer and Morton [11]).

It turns out that the 2 D code with variables v and Θ needs considerably more computation time, mainly for the Rosenbluth potential g (v,Θ). The reason is that an integration over v' and Θ' has to be carried out for each v,Θ pair (see Eq.(4)). The complete elliptic integral $E(\frac{p}{q})$ in Eq. (4) is calculated by a hypergeometric function up to $(\frac{p}{q})^{18}$ in order to save computation time.

/10

3. DISCUSSION OF RESULTS

In this section we present results obtained from applying the Fokker-Planck model to the ionization zone of the tokamak boundary. As mentioned above, in this region drifts as well as sources and sinks due to ionization and charge exchange of D atoms serve as possible causes of distortions of the Maxwellian ion distribution.

An expansion of the drift-kinetic equation (Eq.(1)) in powers of ρ_{pi}/l [6], where ρ_{pi} is the ion gyroradius in the poloidal field and l is the scale length for macroscopic parameters, shows that the zeroth-order contributions result from $\left(\frac{\partial f}{\partial t}\right)_c$ and S, while the term $\vec{v}_d \cdot \vec{\nabla} f$ enters only in the first-order equation of f. Since $\rho_{pi}/l \lesssim 10^{-2}$ holds for typical parameters in the ionization zone (T_i = 50 eV, B $\gtrsim$ 20 kG, l = 50 cm), the drifts produce only very small deviations from the zeroth-order distribution, which is a Maxwellian in the case S = 0. The situation is different, however, with not to small sources and sinks S , which are able to maintain marked deviations from Maxwellians.

Most of the computations were done with Franck-Condon neutrals from walls and limiters which have an isotropic velocity distribution (Maxwellian with T_o = 3 eV)[+]. We therefore apply the fast 1D version of the code using the explicit scheme described in chapter 2.4. Stationary solutions of Eq.(2) were found for various $\frac{n_o}{n}$ and $T_e = \overline{T_i}$, where $\overline{T_i}$ is the average kinetic ion energy. They are reached at a physical time about four times as large as the classical ion-ion collision time. In Fig. 1 steady-state ion distributions $F = \frac{1}{n} f\left(\frac{v}{v_{th}}\right)$ are plotted versus $\frac{v}{v_{th}}$ for $\langle \sigma_i v_e \rangle$ = 0, $T_e = \overline{T_i}$ = 20 eV and various $\frac{n_e}{n}$ ratios. The Maxwellian distribution f_M corresponds to $\frac{n_e}{n}$ = 0. For all curves of a figure the particle number and energy have been kept fixed. It can be seen that non-Maxwellian distributions are produced by sources and sinks due to charge exchange alone. In this case without ionization stationary solutions are obtained

[+] Backscattering of outflowing deuterons produces different neutral particle distributions.

/11

even with S_d = o (see Eq.(2). Figures 2 and 3 show that larger differences from f_M result if both ionization and charge exchange are taken into account. Obviously, for not too small $\frac{n_o}{n}$ ratios considerable deviations from Maxwellians are produced by the influx of cold neutrals. For $T_e = \overline{T_i}$ = 20 eV a normalized deviation defined as $\eta = \frac{f(o) - f_M(o)}{f_M(o)}$ of about 0.1, which is still large compared with the contribution of the drifts, results for $\frac{n_o}{n}$ = 0.013. At temperatures $T_e = \overline{T_i}$ = 50 eV, which are more realistic for the ionization zone (e.g. in TFR 600), significantly smaller $\frac{n_o}{n}$ ratios are sufficient (see Fig. 4). This tendency is continued for $T_e = \overline{T_i}$ = 100 eV (see Fig.5). In Fig. 6 the very sensitive dependence of the $\frac{n_o}{n}$ ratio corresponding to η = 0.1 on the temperature is shown. It results from the decrease of the spreading in velocity space with growing temperature. One can conclude that for realistic temperatures in the ionization zone, such as $T_e = T_i \gtrsim$ 50 to 100 eV, ratios of $\frac{n_o}{n} \gtrsim 2 \cdot 10^{-4}$ to 10^{-3} are sufficient to produce marked deviations from Maxwellians ($\eta \gtrsim 0.1$) in the presence of classical velocity space diffusion. Since the experimental parameters in the ionization zone can be in this range, sources and sinks due to ionization and charge exchange are able to produce large distortions from Maxwellians and can possibly cause microinstabilities in the boundary [12]. These results have been applied to measured profiles of PULSATOR and ASDEX and to profiles computed by the tokamak transport code BALDUR. In the high-density discharges of PULSATOR the $\frac{n_o}{n}$ - values considerably exceed the ratios corresponding to η = 0.1 in the range T_e = 20 to 100 eV. In the ionization zone of ohmically heated ASDEX-discharges, however, the $\frac{n_o}{n}$ - ratios can produce maximum distortions of η = 0.1.

From the figures presented the limitations of a fluid description of the ions become evident. The effect of anomalously frequent collisions was simulated by a coefficient 10 times as large as Γ for a test case with $T_e = \overline{T_i}$ = 20 eV, T_o = 3 eV and $\frac{n_o}{n}$ = 0.2, yielding a reduction of the quantity $f(0) - f_M(0)$ by a factor of 15.

By comparing Figs. 3, 4 and 5 a peaking of distributions at larger temperatures becomes evident. This simply results from the concentration of the 3 eV neutrals and thus of the source to a narrower $\frac{v}{v_{th}}$ range, when the temperature is increased.

Essentially identical stationary solutions were obtained by applying test functions. These computations show that two-temperature distributions with one temperature somewhat above T_o and the other one near T_i represent rather good analytic approximations.

As mentioned above the ion distribution also depends on the different mechanisms of neutral particle production. The largest differences from f_M near v = o result for gas-puffing, i.e. for Franck-Condon neutrals with T_o = 3eV $\ll T_i$ and for recycling. On the other hand, the ion distribution must remain unchanged if neutrals with a distribution identical to f enter the plasma. This can be proved by inserting $\frac{f_o(v)}{n_o} = \frac{f(v)}{n}$ into Eqs.(2), (6) and (7) ($S+S_d$ = o) and has also been numerically confirmed. Thus, rather small distortions of f_M are expected for neutral distributions close to the ion distributions.

In the tokamak boundary roughly equal electron and ion temperatures were measured. Computations with $T_e = \overline{T_i}$ show that the electron-ion collisions contribute only a few per cent to the ion collision operator. The situation is quite different for the test case T_e = 5eV, $\overline{T_i}$ = 20eV and $\frac{n_o}{n}$ = 0.1, where the electron contribution reaches up to 50 % of the total collision term.

4. CONCLUSIONS

Steady-state guiding-centre ion distribution functions were computed for the ionization zone of tokamaks. For typical temperatures $T_e = T_i \gtrsim$ 50 to 100eV and ratios of $\frac{n_o}{n} \gtrsim 2 \cdot 10^{-4}$ to 10^{-3} sources and sinks due to ionization and charge exchange of neutrals from walls and limiters produce marked deviations from Maxwellians ($\eta \gtrsim 0.1$) in the presence of classical velocity space diffusion. The distortions grow with increasing $\frac{n_o}{n}$ and $\frac{T_i}{T_o}$ and possibly cause microinstabilities in the boundary. Both

ionization and charge exchange are able to produce large distortions. The relaxation time to steady-state exceeds the classical ion-ion collision time by a factor of about 4. Drifts yield comparably very small (first-order) deviations from Maxwellian ion distributions.

For $T_e = T_i$ the contributions of electron-ion collisions to the ion collision operator are in the range of a few percent.

Good analytic approximations for the stationary solutions are obtained by two-temperature distributions with one temperature somewhat above T_o and the other one near T_i.

For $T_e = T_i \gtrsim 50$ eV and $\frac{n_o}{n} \gtrsim 10^{-3}$ a fluid description of the ions with classical coefficients is not justified.

ACKNOWLEDGEMENTS

The author appreciates useful discussions with Dr. D.F. Düchs and F. Pohl.

R E F E R E N C E S

[1] Scaturro, L.S., Kusse, B., Nucl.Fus.18, 1717 (1978)

[2] Azumi, M., et al., Nucl.Fus. 18, 1619 (1978)

[3] Gomay, Y., et al., Nucl.Fus. 18, 849 (1978)

[4] Slusher, R.E., Surko, C.M., Phys.Rev. Letters 40, 400 (1978)

[5] Callen,J.D., et al., in Plasma Physics and Controlled Nuclear Fusion Research (Proc. 8th Int. Conf. Brussels, 1980) IAEA - CN - 38/Y-3.

[6] Hinton, F.L., Hazeltine, R.D., Reviews of Modern Physics 48, Part I , 239 (1976)

[7] Waltz, R.E., Burrell, K.H., Nucl.Fus. 17, 1001 (1977)

[8] Marx, K.D., Phys. of Fluids 13, 1355 (1970)

[9] Killeen, J., Mirin, A.A., Rensink, M.E., in "Methods in Computational Physics" 16, 389 (1976)

[10] Pohl, F., IPP Report, to be published.

[11] Richtmyer, R.D., Morton, K.W., in "Difference Methods for Initial-Value Problems", Interscience Publishers New York (1967)

[12] Tang, W.M., Nucl.Fus. 18, 1089 (1978)

F I G U R E C A P T I O N S

FIG. 1. Stationary ion distribution functions $F\left(\frac{v}{v_{th}}\right)$ for $\langle \sigma_i v_e \rangle = 0$, $T_e = \overline{T_i} = 20\text{eV}$ and $T_o = 3\text{eV}$.

FIG. 2. $F\left(\frac{v}{v_{th}}\right)$ for $T_e = \overline{T_i} = 20\text{eV}$, $T_o = 3\text{eV}$ and large $\frac{n_o}{n}$ values.

FIG. 3. $F\left(\frac{v}{v_{th}}\right)$ for $T_e = \overline{T_i} = 20\text{eV}$, $T_o = 3\text{eV}$ and small $\frac{n_o}{n}$ values.

FIG. 4. $F\left(\frac{v}{v_{th}}\right)$ for $T_e = \overline{T_i} = 50$ eV and $T_o = 3\text{eV}$.

FIG. 5. $F\left(\frac{v}{v_{th}}\right)$ for $T_e = \overline{T_i} = 100\text{eV}$ and $T_o = 3\text{eV}$

FIG. 6. $\frac{n_o}{n}$ ratio as a function of $T_e = \overline{T_i}$ for normalized deviation $\eta = 0.1$.

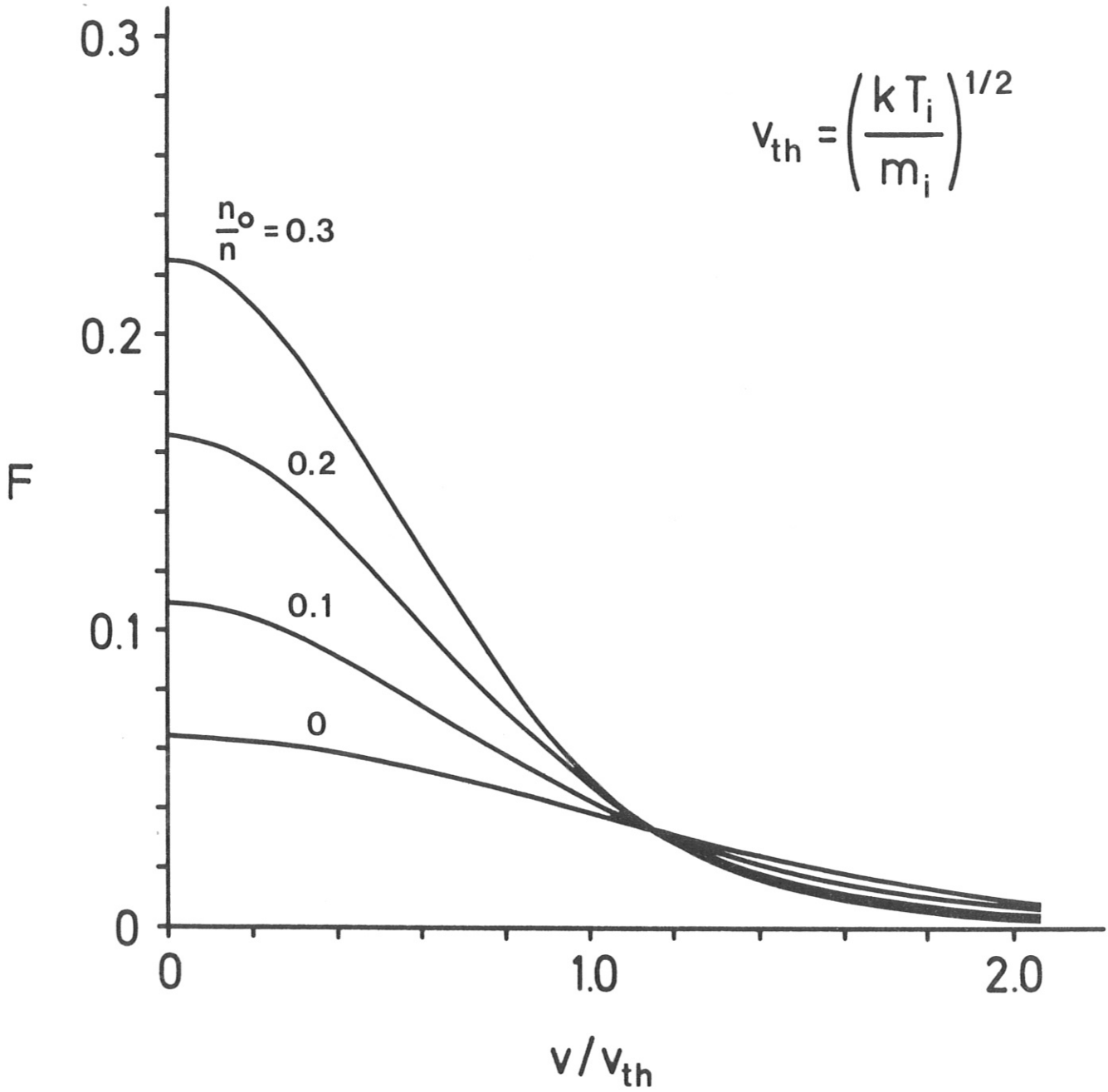
0.3
0.2
0.1
0
F
$v_{th} = \left(\frac{k T_i}{m_i}\right)^{1/2}$
$\frac{n_o}{n} = 0.3$
0.2
0.1
0
0
1.0
2.0
v/v_{th}

Fig. 1

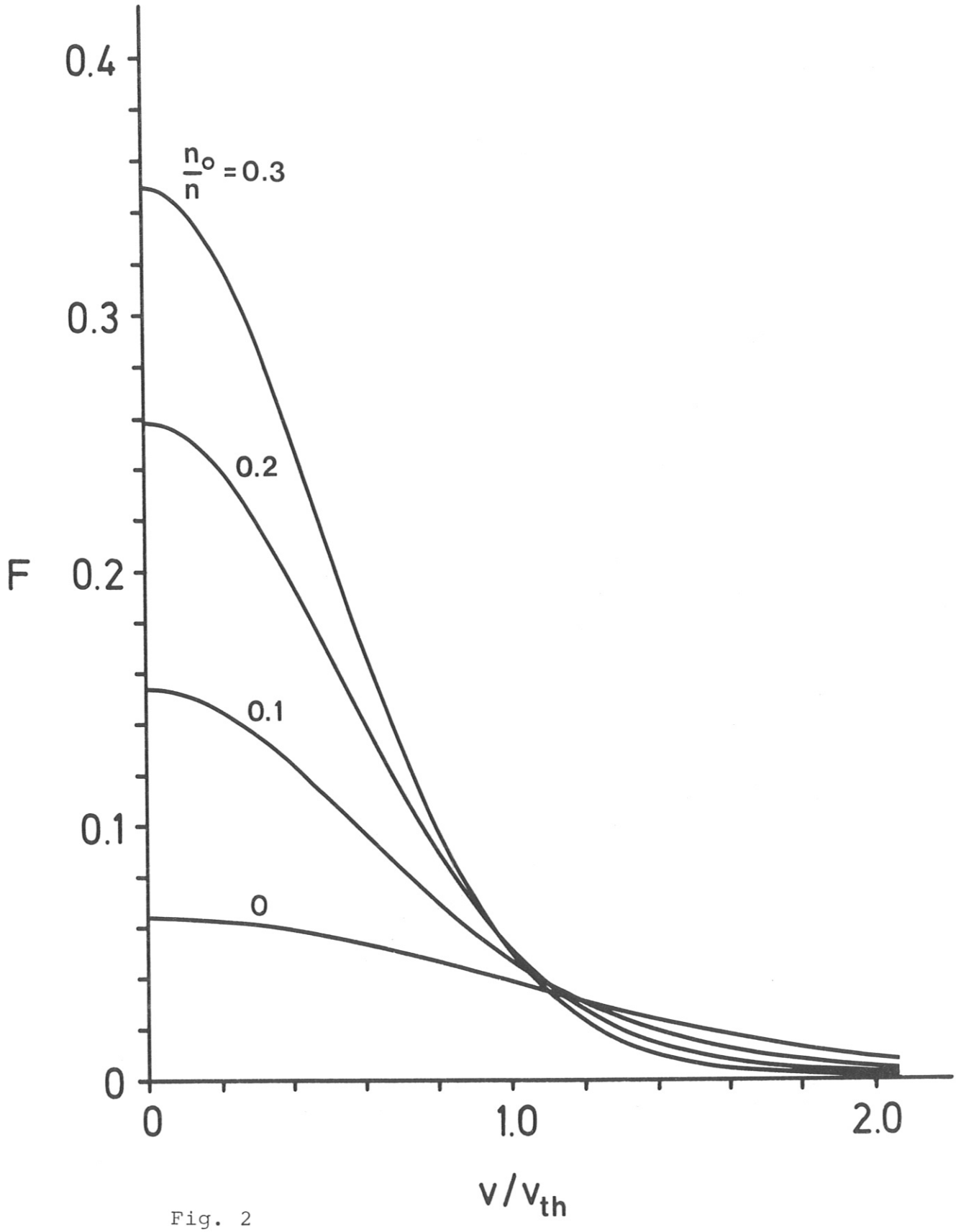

Fig. 2

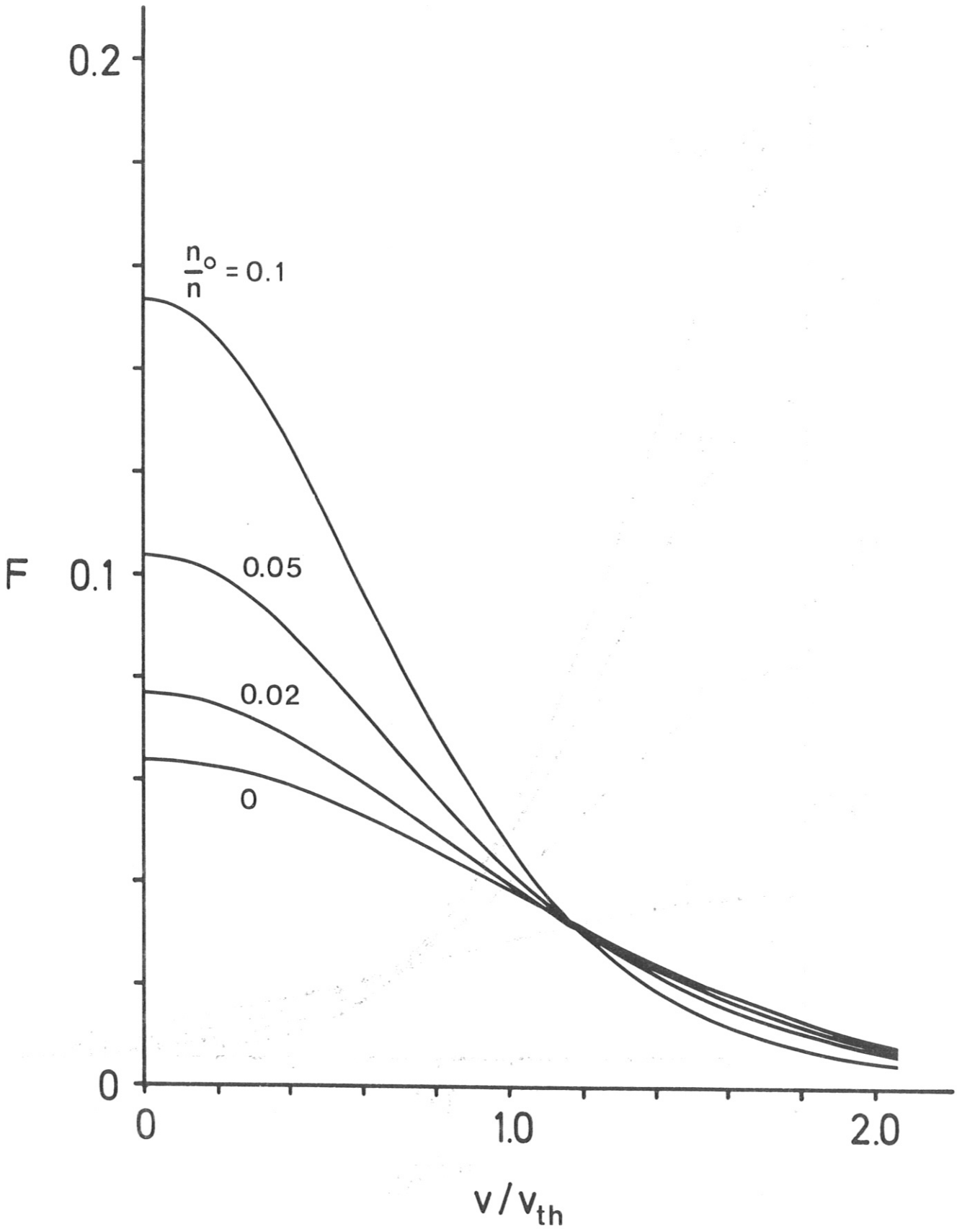

Fig. 3

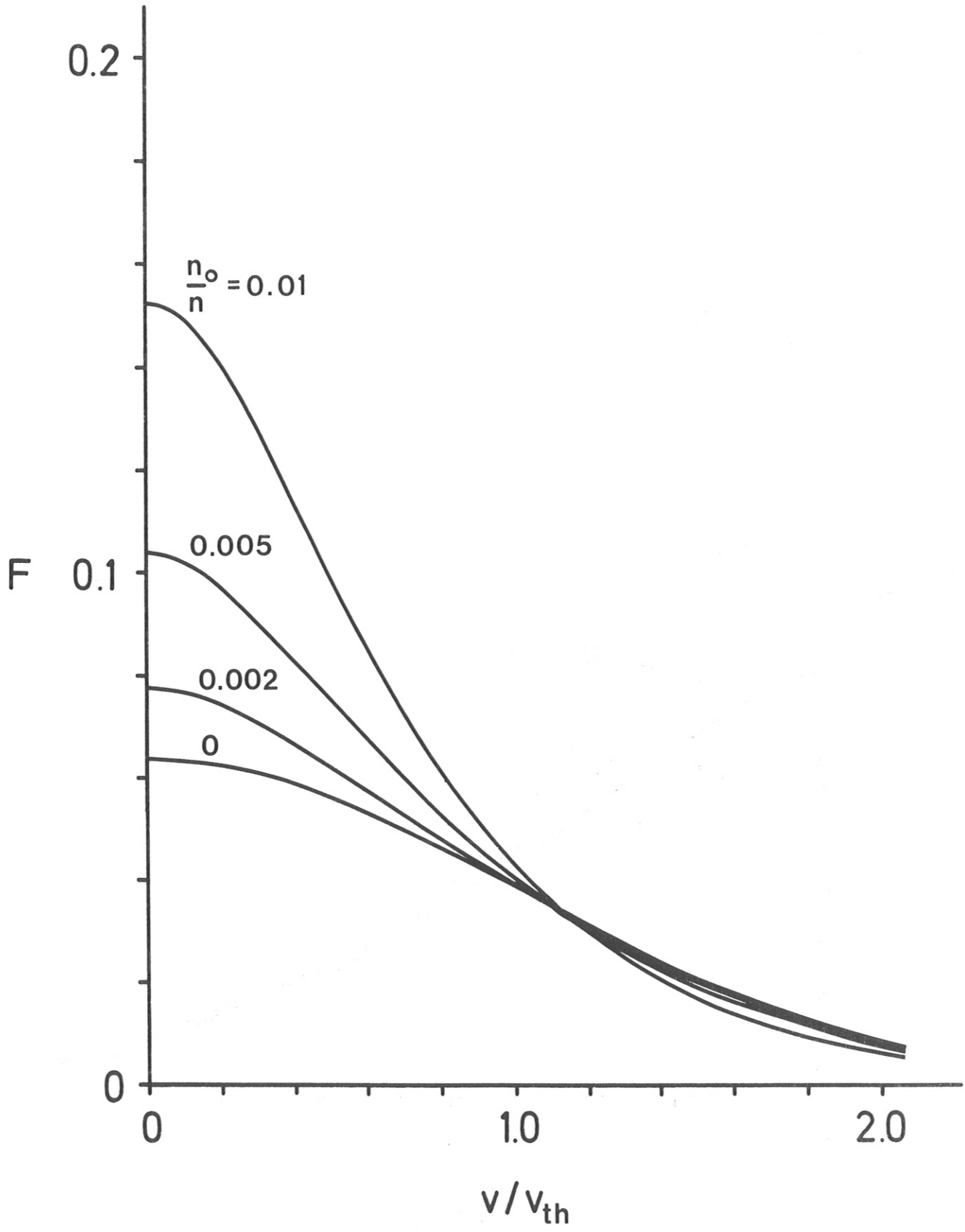

Fig. 4

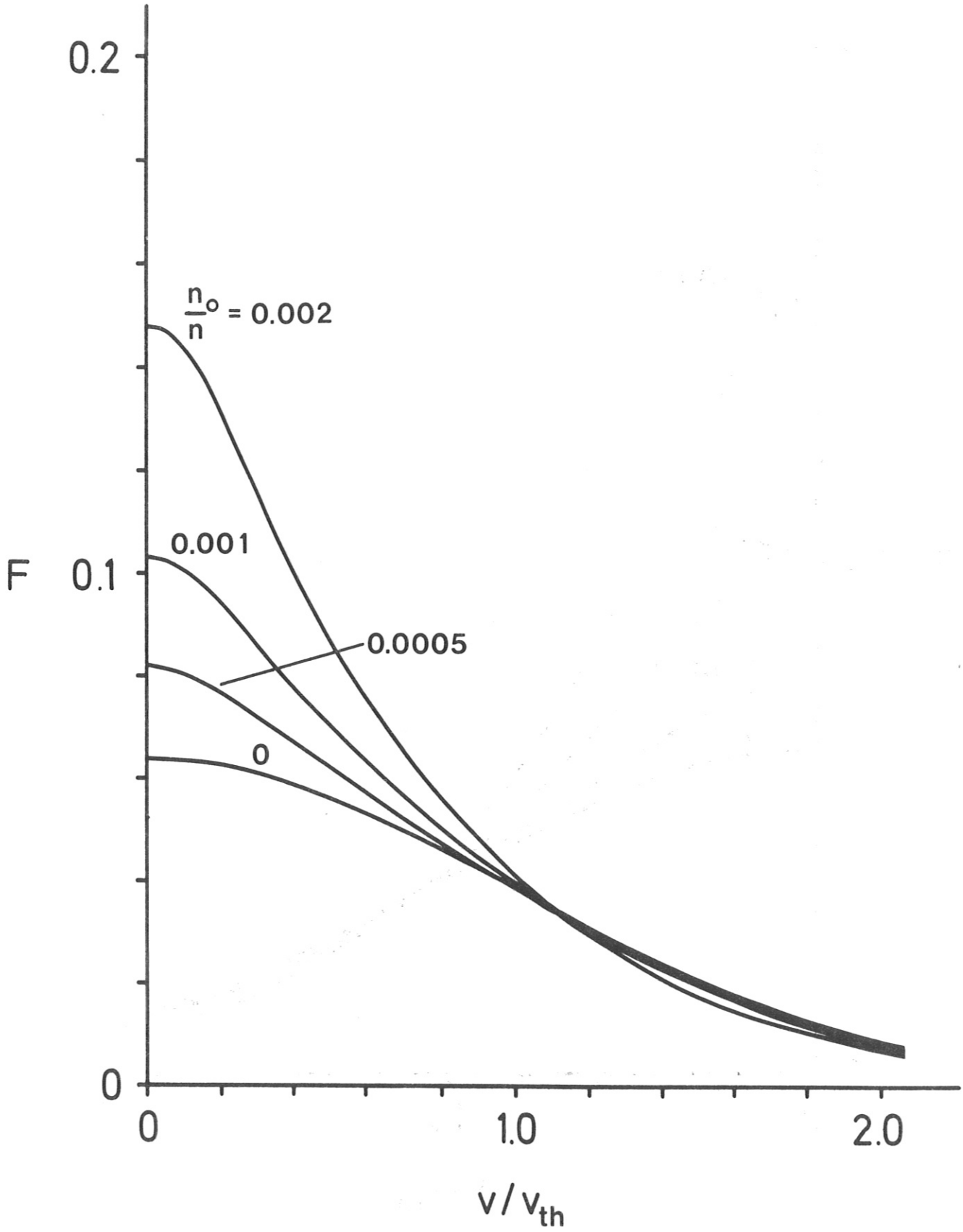

Fig. 5

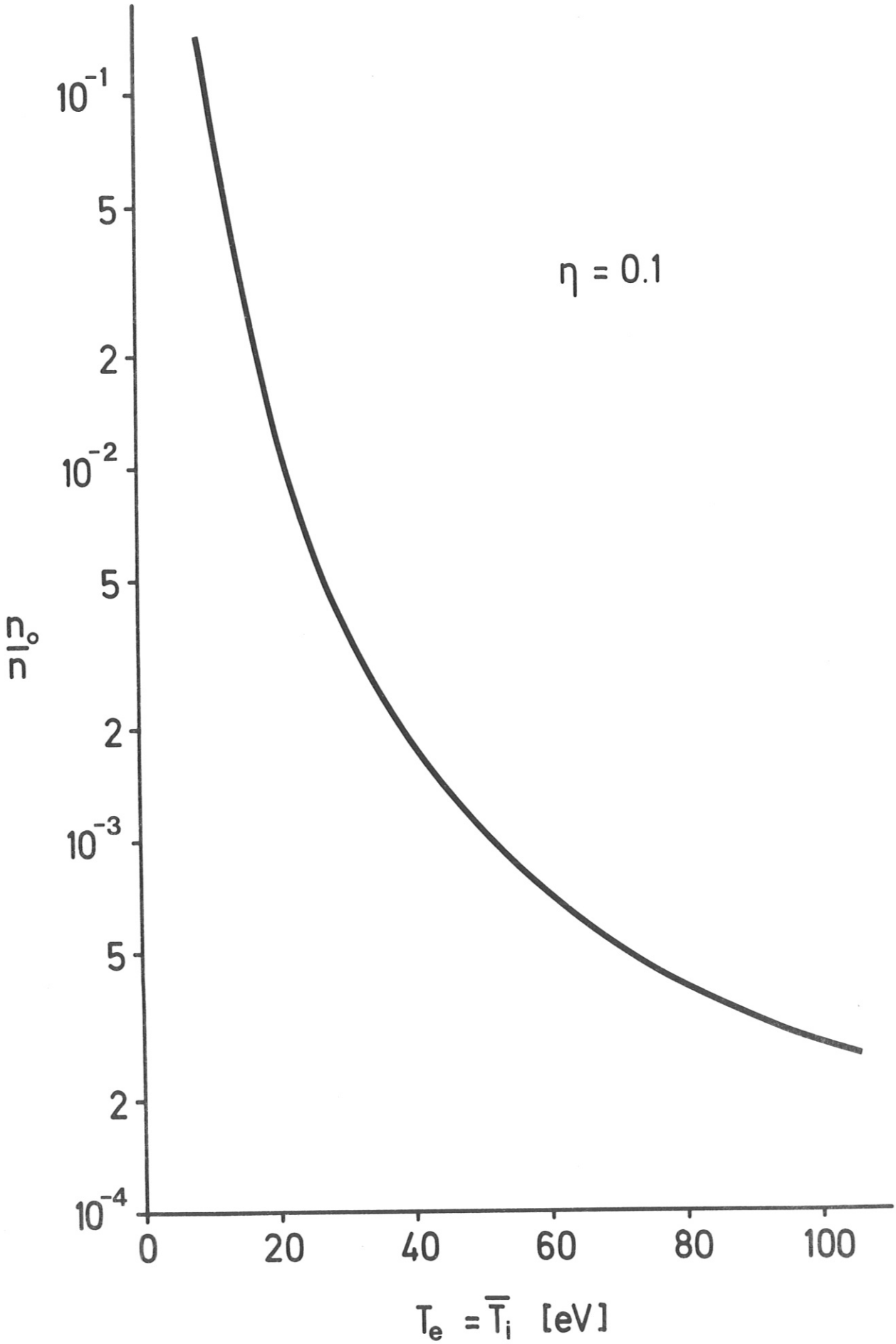
10^{-1}
5
2
10^{-2}
5
2
10^{-3}
5
2
10^{-4}
$\frac{n_o}{n}$
$\eta = 0.1$
0
20
40
60
80
100
$T_e = \overline{T}_i$ [eV]

Fig. 6